Canti *et al*. 10.1073/pnas.0504183102. Vol 102 11230-11235 (2005).

Supporting Information

Supporting Figure 6

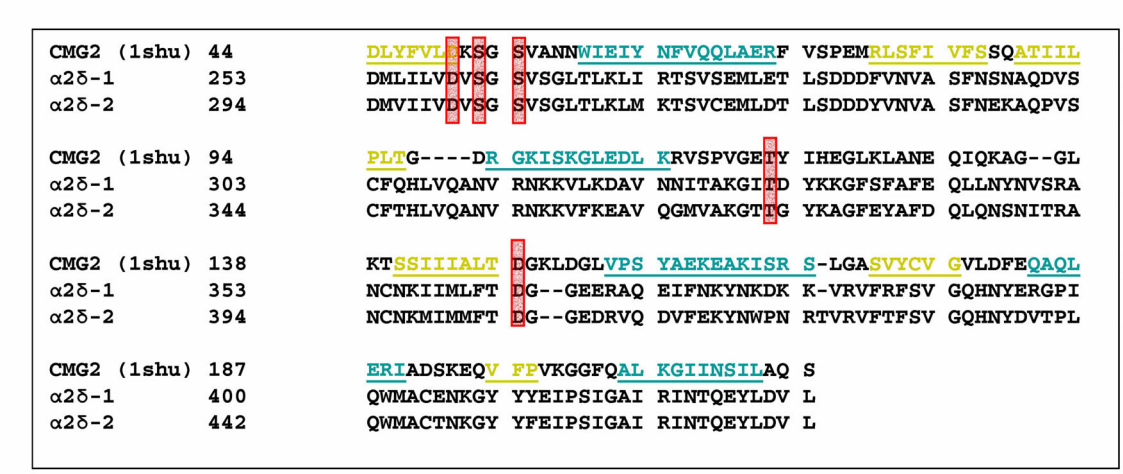

Fig. 6. Structural alignment of the $\alpha_2\delta$-2 VWA domain with other VWA domains. Structural alignment of the VWA domains of $\alpha_2\delta$-1, $\alpha_2\delta$-2, and CMG2 (1shu) generated by the program fugue. Residues of the MIDAS motif are shown in vertical red boxes. Structural elements within the CMG2 VWA domain are underlined (α-helix, cyan; β-strand, yellow).

Supporting Figure 7

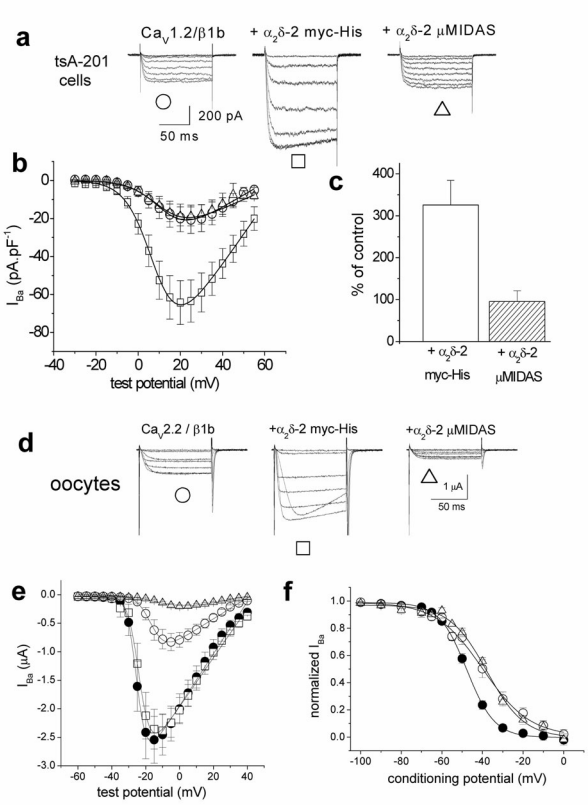

Fig. 7. Comparison of the effects of $\alpha_2\delta$-2 and $\alpha_2\delta$-2 μMIDAS on $Ca_V1.2$ currents in tsA-201 cells and $Ca_V2.2$ current properties in *Xenopus* oocytes. (*a*) $Ca_V1.2/\beta1b$ was expressed with the various $\alpha_{2\delta}$-2 constructs in tsA-201 cells, with 10 mM Ba^{2+} as charge carrier (see *Experimental Procedures*). Representative current traces were elicited between –10 and +25 mV in 5-mV steps from a holding potential of –90 mV for $Ca_V1.2/\beta1b$ (*Left*), $Ca_V1.2/\beta1b/\alpha_2\delta$-2 myc-His (*Center*), and $Ca_V1.2/\beta1b/\alpha_2\delta$-2 μMIDAS (*Right*). (*b*) Average current–voltage (*I–V*) relationships for the three experimental conditions. ○, $Ca_V1.2/\beta1b$ (n = 7); □, +$\alpha_2\delta$-2 myc-His (n = 6) and Δ, +$\alpha_2\delta$-2 μMIDAS (n = 8). (*c*) Bar chart at +20 mV (calculated as a percentage of the mean control $Ca_V1.2/\beta1b$ currents) for +$\alpha_2\delta$-2 myc-His (white bar) and +$\alpha_2\delta$-2 μMIDAS (hatched bar). The number of determinations is as in *b*. (*d*) $Ca_V2.2/\beta1b$ was expressed with the various $\alpha_2\delta$-2 constructs in *Xenopus* oocytes. Representative current traces elicited between –50 and +10 mV in 10-mV steps from a holding potential of –90 mV for $Ca_V2.2/\beta1b$ (*Left*), $Ca_V2.2/\beta1b/\alpha_2\delta$-2 myc-His (*Center*), and $Ca_V2.2/\beta1b/\alpha_2\delta$-2 μMIDAS (*Right*). Traces and *I–V* relationship were obtained by using 2 mM Ba^{2+}as a charge carrier (see *Experimental Procedures*). Similar data were obtained with 5 mM and 40 mM Ba^{2+}. (*e*) Average *I–V* relationships for four different experimental conditions. ○, $Ca_V2.2/\beta1b$ (n = 25); ●, +$\alpha_2\delta$-2 (n = 17); □, +$\alpha_2\delta$-2 myc-His (n = 30); and Δ, +$\alpha_2\delta$-2 μMIDAS (n = 17). (*f*) Steady-state inactivation curves for test pulses to –10 mV, after a 15-s conditioning prepulse of between –110 and 0 mV in 10-mV steps. ○, $Ca_V2.2/\beta1b$ (n = 6); ●, +$\alpha_2\delta$-2 (n = 7); and Δ, +$\alpha_2\delta$-2 μMIDAS (n = 4). The charge carrier was 40 mM Ba^{2+}. The data were fit with a single Boltzmann equation. The mean V_{50} values for inactivation were –39.7, –47.6, and –37.8 mV, respectively.

Supporting Figure 8

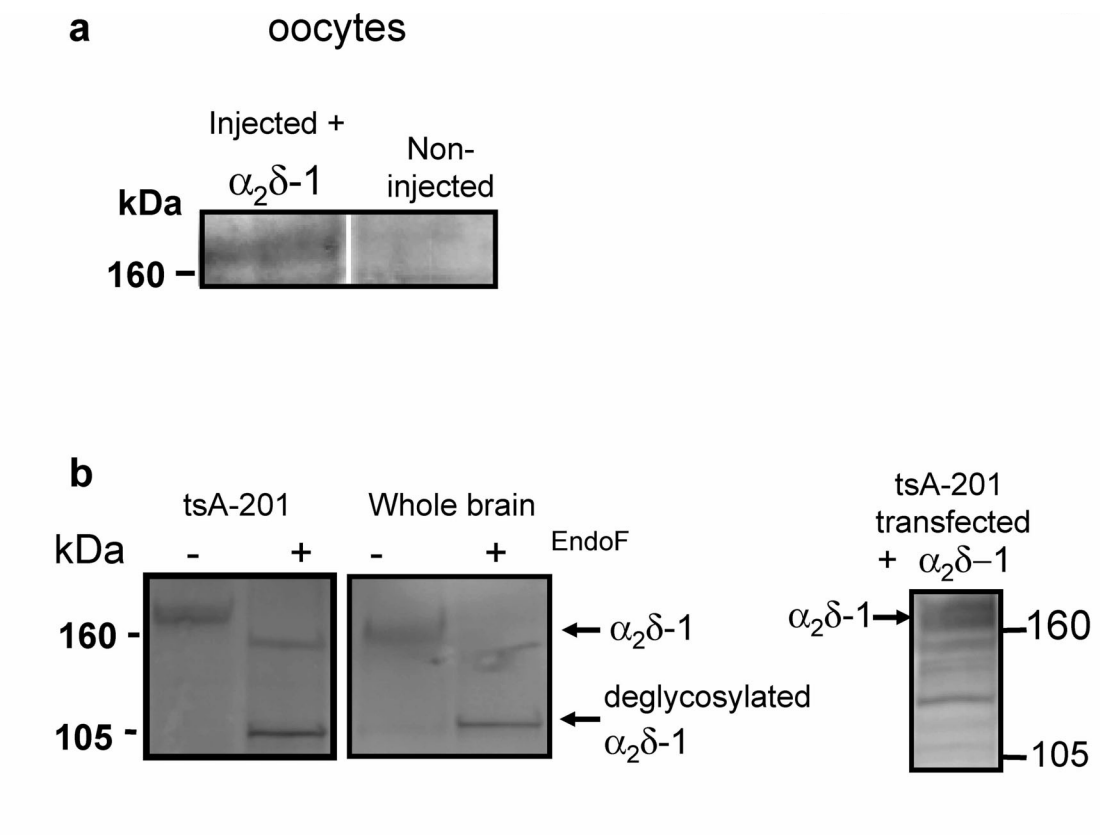

Fig. 8. Detection of $\alpha_2\delta$-1 in tsA-201 cells but not in *Xenopus* oocytes. The anti-$\alpha_2\delta$-1 Ab used in this figure is a polyclonal Ab raised against amino acids 27–41of rat $\alpha_2\delta$-1. (*a*) Western blot for injected $\alpha_2\delta$-1 as a positive control (*Left*) and lack of endogenous $\alpha_2\delta$-1 (*Right*) in lysate from an individual *Xenopus* oocyte (representative of at least 10 oocytes from several different batches). (*b*) Western blot demonstrating the presence of endogenous $\alpha_2\delta$-1 in a purified tsA-201 cell membrane sample (*Left*), compared with a sample from whole brain treated identically (*Center*). Samples contain DTT (10 mM) and have either been treated (+) or not (–) with endoglycosidase F (2 units). The upper arrow indicates the position of the glycosylated α_2 moiety of $\alpha_2\delta$-1, and the lower arrow indicates the position of the major deglycosylated band, with the expected protein molecular mass of 105 kDa. Samples were run on a 3–8% Tris acetate gel. (*Right*) A sample of whole cell lysate of tsA-201 cells transfected with $\alpha_2\delta$-1, as a positive control.

Supporting Figure 9

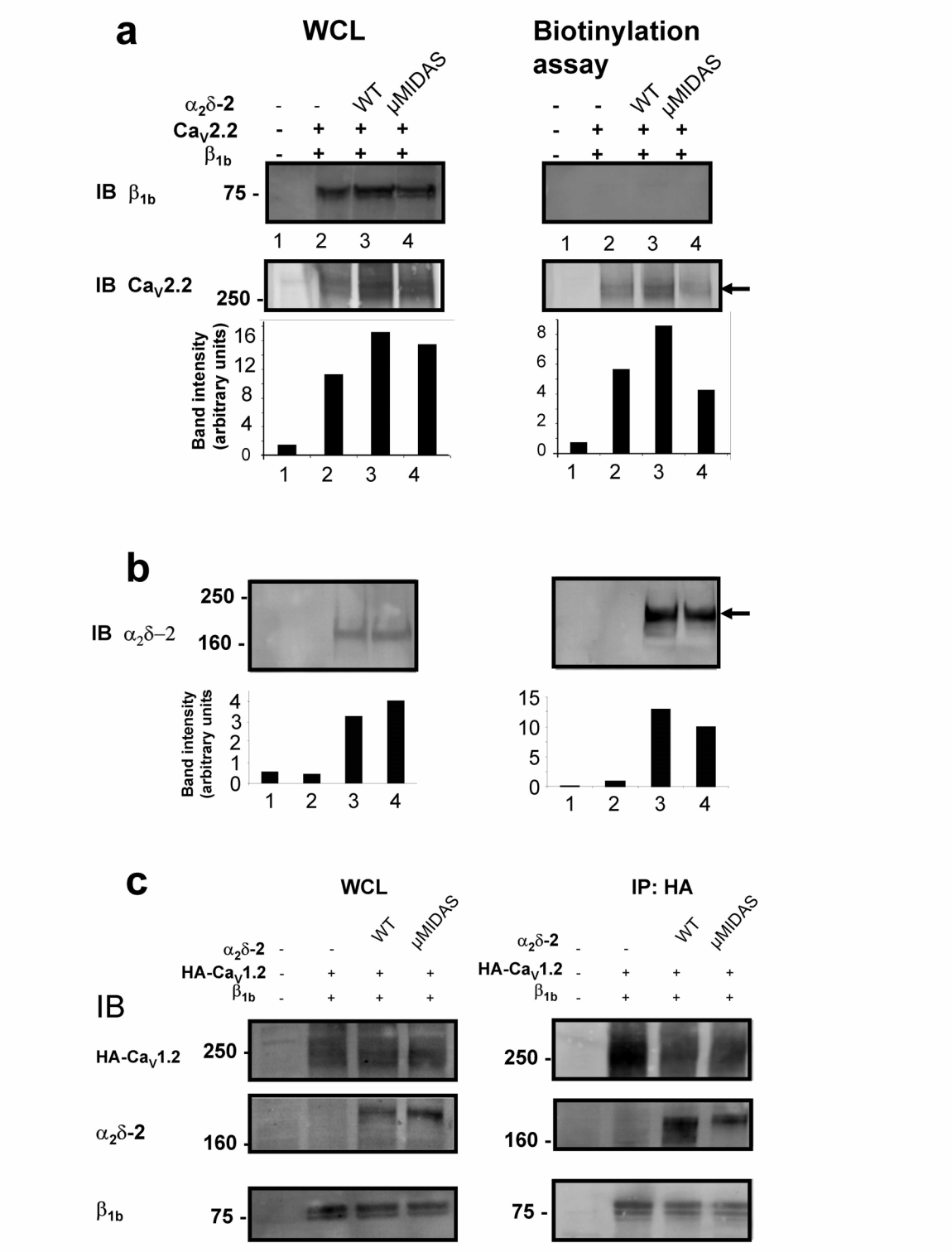

Fig. 9. Cell-surface expression of $Ca_V2.2$ in Cos-7 and tsA-201 cells. (*a Left*) Comparison of the expression in whole-cell lysates (WCL) of tsA-201 cells of $Ca_V\beta1b$ (*Upper*) and $Ca_V2.2$ (*Lower*). Shown are empty-vector-transfected cells (lane 1), $Ca_V2.2/\beta1b$ alone (lane 2), $Ca_V2.2/\beta1b/\alpha_2\delta$-2

(lane 3), and $Ca_V2.2/\beta1b/\alpha_2\delta$-2 μMIDAS (lane 4). (*Right*) Isolation of cell-surface biotinylated proteins from the same experiment. The arrow indicates a lower level of biotinylated $Ca_V2.2$ in the presence of $\alpha_2\delta$-2 μMIDAS. The data presented are representative of three independent experiments. The upper blot indicates the absence of biotinylated β1b. The lack of biotinylation of the intracellular β1b confirms that no intracellular proteins have been detected. Blots were quantified by using the program Imagequant, and the intensity is shown (in the bar chart) after the subtraction of an equivalent background from the same lane. The percentage at the cell surface was calculated as (intensity of biotinylated $Ca_V2.2$ band)/(intensity of WCL $Ca_V2.2$ band × fraction of total sample loaded). The percentage was 3.7%, 3.9%, and 2.0% for $Ca_V2.2/\beta1b$ alone, $Ca_V2.2/\beta1b/\alpha_2\delta$-2, and $Ca_V2.2/\beta1b/\alpha_2\delta$-2 μMIDAS, respectively. The data are representative of three experiments. (*b Left*) Comparison of the expression in WCL of Cos-7 cells, $\alpha_2\delta$-2, and $\alpha_2\delta$-2 μMIDAS. Shown are empty-vector-transfected (lane 1), $Ca_V2.2/\beta1b$ alone (lane 2), $Ca_V2.2/\beta1b/\alpha_2\delta$-2 (lane 3), and $Ca_V2.2/\beta1b/\alpha_2\delta$-2 μMIDAS (lane 4). (*Right*) Isolation of cell-surface biotinylated proteins from the same experiment. The arrow indicates the level of biotinylated $\alpha_2\delta$-2 and $\alpha_2\delta$-2 μMIDAS in the presence of $Ca_V2.2$. The data are representative of three independent experiments. A lower percentage of the total $\alpha_2\delta$-2 μMIDAS was biotinylated and, therefore, expressed at the cell surface compared with WT $\alpha_2\delta$-2, when coexpressed with $Ca_V2.2/\beta1b$ but not when expressed without it (see Fig. 1*c*). The percentage of the total WT $\alpha_2\delta$-2 or μMIDAS $\alpha_2\delta$-2 present at the cell surface was calculated to be 31.8% and 18.9%, respectively, in this experiment. In two similar experiments performed in tsA-201 cells, there was an average at the cell surface of 19.0% and 10.9%, respectively. Thus, all experiments showed a 40–50% reduction in the expression of $\alpha_2\delta$-2 μMIDAS at the cell surface, relative to WT $\alpha_2\delta$-2 when both were coexpressed with $Ca_V2.2/\beta1b$. (*c*) tsA-201 cells were cotransfected with HA-$Ca_V1.2$, β1b, and $\alpha_2\delta$-2 or $\alpha_2\delta$ μMIDAS, and lysates were used for immunoprecipitation with anti-HA Ab. The WCL (*Left*) and immunoprecipitate (IP) (*Right*) were blotted with anti HA (*Top*), α_2(102-117) (*Middle*), and β 1b (*Bottom*). The blots show that $Ca_V1.2$ can coimmunoprecipitate with both WT and MIDAS mutant $\alpha_2\delta$-2. In a separate experiment, a control membrane protein, $K_V3.1b$, did not coimmunoprecipitate with $\alpha_2\delta$-2 (data not shown).

Supporting Figure 10

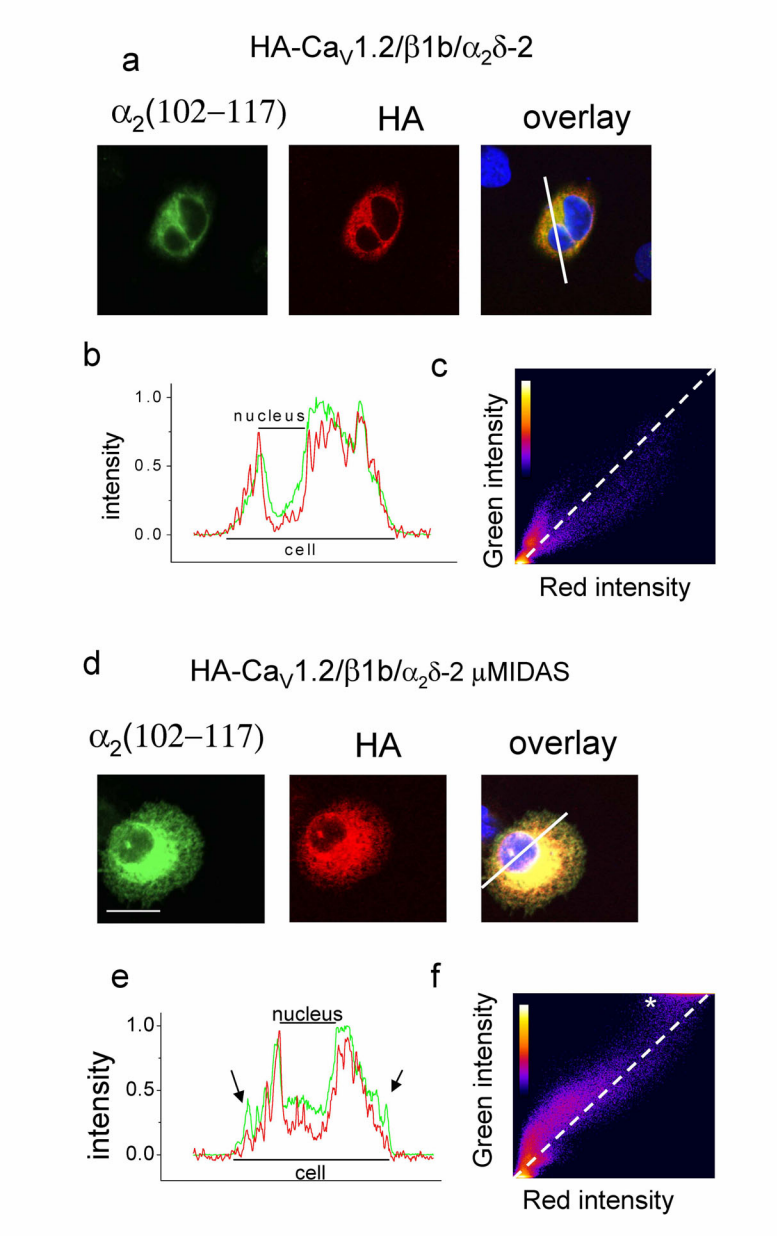

Fig. 10. Additional examples of coexpression of HA-Ca$_V$1.2 with β1b and α$_2$δ-2 or α$_2$δ-2 μMIDAS in Cos-7 cells. Shown are the coexpression of HA-Ca$_V$1.2 with β1b and either α$_2$δ-2 (*a*) or α$_2$δ-2 μMIDAS (*d*). The line on the merged images (overlay) indicates where the line scans in *b* and *e* were taken. [Scale bar, 20 μm (*a* and *d*).]. The arrows in *e* indicate regions where Ca$_V$1.2 immunoreactivity is absent from the periphery of the cell. (*c* and *f*) Pixel-intensity-correlation plots for nonzero pixels in the entire image, shown for α$_2$δ-2 (*c*) or α$_2$δ-2 μMIDAS (*f*) (green, *y* axis) vs. Ca$_V$1.2 (red, *x* axis). The pixel number calibration bar is shown on each plot. The asterisk in *f* indicates an additional region of high-intensity colocalization. The diagonal dotted line indicates theoretical colocalization.

Supporting Figure 11

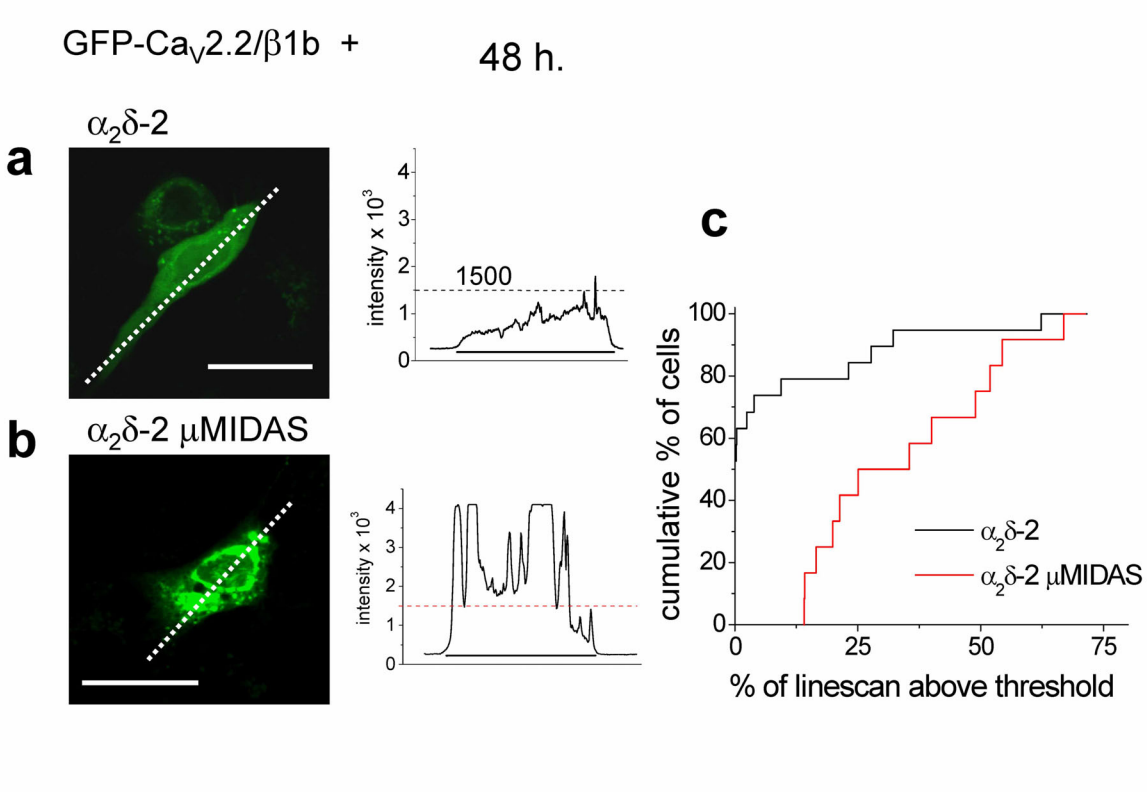

Fig. 11. Comparison of the effect of $\alpha_2\delta$-2 and $\alpha_2\delta$-2 μMIDAS on the distribution of GFPCa$_V$2.2 channels in Cos-7 cells at 48 h. (*Left*) Localization of GFP-Ca$_V$2.2 in Cos-7 cells, when coexpressed with β1b and either $\alpha_2\delta$-2 (*a*) or $\alpha_2\delta$-2 μMIDAS (*b*) 48 h after transfection. Dotted white lines correspond to the positions of the line scans shown to the right. (Scale bars, 50 μm.) (*Right*) Line scans of GFP-Ca$_V$2.2 fluorescence were analyzed through the nucleus of the cells shown. The horizontal dotted line shows the 1,500 intensity threshold (12-bit images), and the line beneath the scans shows the extent of the cell. (*c*) For cells, including those on the left, at 48 h after transfection, line scans of GFP-Ca$_V$2.2 fluorescence were analyzed through the nucleus of $\alpha_2\delta$-2- (n = 19, black line) and $\alpha_2\delta$-2 μMIDAS-containing cells (n = 12, red line), and the percentage of the line scan within the cell above the 1,500 intensity threshold was determined. The plot represents a cumulative frequency histogram, showing the greater proportion of high-intensity GFP-Ca$_V$2.2 fluorescence regions in $\alpha_2\delta$-2 μMIDAS (mean 38.8 ± 5.7%) compared with $\alpha_2\delta$-2-containing cells (mean 12.3 ± 5.0%; P = 0.002).

Supporting Figure 12

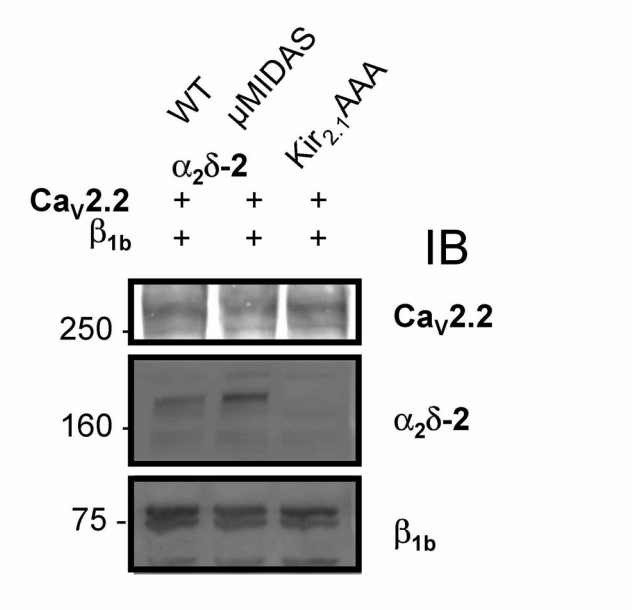

Fig. 12. Expression of GFP-$Ca_V2.2$ in NG108-15 cells. NG108-15 cells were transfected with the constructs shown and differentiated as for the experiments depicted in Fig. 5. Cell lysates were immunoblotted (IB) for $Ca_V2.2$, $\alpha_2\delta$-2, and β1b. No systematic difference in the expression of GFP-$Ca_V2.2$ was observed.

Supporting Methods

Structural Modeling. Suitable templates for modeling were selected from available structures by using the program fugue (1). Models were generated according to the structural alignments from fugue by using the program modeller4 (2). Validation of the model was performed by procheck 3.5 (3). Fig. 1 was generated and rendered by using pymol (DeLano Scientific, San Carlos, CA). In validation, the $\alpha_2\delta$-1 and $\alpha_2\delta$-2 Von Willebrand factor-A (VWA)-domain models received overall G-factors of –0.14 and –0.04, respectively, with 85.4% and 87%, respectively, of their residues in the most-favored regions of the Ramachandran plot and only one residue in a disallowed region, indicating that both models are stereochemically and geometrically acceptable.

CD. GST-fusion proteins of WT $\alpha_2\delta$-2 and $\alpha_2\delta$-2 μMIDAS (metal-ion-dependent adhesion site) VWA domains were expressed in *Escherichia coli* and purified by standard techniques to 0.5 mg/ml. Averaged CD spectra ($n = 5$) were obtained for these two proteins and for GST alone, and the spectra of the $\alpha_2\delta$ VWA domains was obtained by subtraction. The program continll was used for analysis of CD spectra, as described in ref. 4.

Construction and Heterologous Expression of cDNAs. The $\alpha_2\delta$-2 μMIDAS myc-His construct was made by standard molecular biological techniques and verified by DNA sequencing. Mammalian cell lines were transfected with cDNAs for rabbit $Ca_V2.2$ (D14157 without 3' UTR), GFP-$Ca_V2.2$ (5), or HA-tagged $Ca_V1.2$ (6) in conjunction with rat β1b (7) and mouse $\alpha_2\delta$-2 (AF247139) (8), $\alpha_2\delta$-2 myc-His, or its mutated construct $\alpha_2\delta$-2 μMIDAS myc-His. The cDNAs were subcloned into the pMT2 vector for expression in tsA-201 or Cos-7 cells or into pRK5 or pcDNA3.1 for NG108-15 cells. The cDNA for GFP (mut3 GFP) (9) was included in the transfection to identify transfected cells from which electrophysiological recordings were made. Transfection was performed as described in ref. 10. For expression in *Xenopus* oocytes, cDNAs were injected intranuclearly, as described in ref. 11. In control experiments, in which $\alpha_2\delta$-2 was omitted, the ratio was made up as stated, with buffer or a control Kir2.1 channel mutated so that it does not pass current (Kir2.1-AAA), with equivalent results (10, 12). For differentiation, NG108-15 cells were cultured as described in ref. 10 and differentiated 3 h after plating by replacing the growth medium with one containing only 1% FCS and no aminopterine with prostaglandin E_1 (10 μM) and 3-isobutyl-1-methylxanthine (50 μM). Transfection was performed 1 h after differentiation by using the transfection reagent Fugene (Roche Diagnostics, Lewes, U.K.).

Gabapentin-Binding Assay. Binding of [^{3}H]gabapentin to Cos-7 cell-membrane preparations expressing either WT $\alpha_2\delta$-2 or $\alpha_2\delta$-2 μMIDAS myc-His (and mut3 GFP to determine transfection efficiency) was carried out in a final volume of 250 μl at room temperature for 45 min. Membranes (50 μg per tube) were incubated with various concentrations of [^{3}H]gabapentin [36 Ci/mmol (1 Ci = 37 GBq), Tocris Cookson, Bristol, U.K.] in 10 mM Hepes/KOH, pH 7.4, then rapidly filtered through grade B glass microfiber filters (Whatman, Brentford, U.K.) presoaked with 0.3% polyethyleneimine. The filters were washed three times with 3 ml of ice-cold 50 mM Tris·HCl, pH 7.4, and the amount of bound [^{3}H]gabapentin was determined by scintillation counting. Concentrations of [^{3}H]gabapentin >50 nM were achieved by adding nonradioactive gabapentin and correcting the specific binding by the dilution factor, as described in ref. 13. Nonspecific binding was determined in the presence of 20 μM nonradioactive gabapentin. Three

independent experiments were performed, each in triplicate, and data were analyzed by fitting specific binding to the equation for a rectangular hyperbola.

Immunocytochemistry. The method used is essentially as described in ref. 14, except for cell-surface labeling (primary Ab was applied for 1 h at 37°C before washing twice in PBS) and fixation. Cells were fixed with 4% paraformaldehyde in PBS for 5 min at room temperature. For labeling intracellular epitopes, cells were permeabilized by incubating twice for 7 min in a 0.02% solution of Triton X-100 in Tris-buffered saline (TBS); otherwise, cells were washed twice with TBS for the same time period. The primary anti-$\alpha_2\delta$ Abs (15, 16) were used at 1–2 $\mu g \cdot ml^{-1}$, followed by the secondary FITC-conjugated goat anti-rabbit Ab (1:500, Sigma). A rat monoclonal anti-HA Ab (Roche) was used at 0.2 $\mu g \cdot ml^{-1}$ with a biotinylated anti-rat IgG (0.6 $\mu g \cdot ml^{-1}$, Sigma), followed by streptavidin-Texas red (2 $\mu g \cdot ml^{-1}$, Molecular Probes). In some experiments, the nuclear dye DAPI (500 nM, Molecular Probes) was also used to visualize the nucleus. Cells were mounted in VECTASHIELD (Vector Laboratories) to reduce photobleaching and examined on a Zeiss LSM confocal laser scanning microscope with a magnification ×40 (1.3 NA) or magnification ×63 (1.4 NA) oil-immersion objective. Optical sections were 1 μm. Photomultiplier settings were kept constant in each experiment, and all images were scanned sequentially. For imaging GFP in live cells, glass-bottomed dishes (MatTek, Ashland, MA) were mounted in a humidified chamber on the microscope and perfused with 5% CO_2. Image processing was performed by using the programs metamorph (Universal Imaging, Downington, PA) and imagej (http://rsb.info.nih.gov/ij). Data illustrated are representative of >10 cells from at least three independent experiments.

Biotinylation Assay. At 48 h after transfection, cells were rinsed three times with PBS and incubated with PBS containing 0.5 mg/ml Sulfo-NHS-SS-Biotin (Pierce) for 30 min at room temperature. The biotin solution was removed and replaced with PBS containing 100 mM glycine for 2 min at room temperature to quench the reaction. The cells were gently rinsed three times with PBS and lysed as described above. One-tenth of the cell lysate was loaded onto a 3–8% Tris-acetate gel to determine total protein expression. Biotinylated proteins were precipitated by adding 50 μl of streptavidin-agarose beads (Pierce) and were incubated overnight at 4°C. The streptavidin-agarose beads were washed three times and incubated with 100 mM DTT for 30 min at room temperature, followed by resuspension in 2× Laemmli sample buffer. Eluted proteins were resolved by SDS/PAGE.

Deglycosylation. Endoglycosidase F digestion of biotinylated or native proteins was performed by using a kit from New England Biolabs (Hitchin, U.K.) according to the manufacturer's instructions.

Immunoprecipitation and Immunoblotting. Cell lysates were generated from Cos-7 or tsA-201 cells in ice-cold lysis buffer containing 1% Igepal for 30 min on ice. For immunoprecipitation, lysates were incubated overnight at 4°C with the anti-$Ca_V2.2$ or anti-HA Ab and then for 1 h with protein A- (or G-) Sepharose beads (Sigma). The pellets were washed three times with ice-cold lysis buffer containing 0.2% Igepal and resuspended in SDS sample buffer. Eluted immunoprecipitates or whole-cell lysates were separated by SDS/PAGE and analyzed by immunoblotting. SDS/PAGE-resolved samples were transferred to poly(vinylidene difluoride) membranes and probed with primary anti-$Ca_V2.2$ (5), anti-$\alpha2$(102–117) (16), anti-β1b (17), or

commercial anti-HA or anti-GFP Abs and horseradish-peroxidase-conjugated secondary Abs, followed by enhanced chemiluminescence detection.

Electrophysiology. Calcium-channel expression in tsA-201 cells was investigated by whole-cell patch-clamp recording, essentially as described in ref. 18. The internal (pipette) and external solutions and recording techniques were similar to those described in ref. 19. The patch-pipette solution contained 140 mM Cs-aspartate, 5 mM EGTA, 2 mM $MgCl_2$, 0.1 mM $CaCl_2$, 2 mM K_2ATP, and 10 mM Hepes, pH 7.2 (310 mOsm with sucrose). The external solution for recording Ba^{2+} currents contained 150 mM tetraethylammonium (TEA) Br, 3 mM KCl, 1.0 mM $NaHCO_3$, 1.0 mM $MgCl_2$, 10 mM Hepes, 4 mM glucose, and 10 mM $BaCl_2$, pH 7.4 (320 mosM with sucrose). For recording Na^+ currents through Ca^{2+} channels, Ba^{2+} and Mg^{2+} were replaced by Na^+. The solution contained 100 mM NaBr, 60 mM TEA Br, 3 mM KCl, 1.0 mM $NaHCO_3$, 10 mM Hepes, 4 mM glucose, and 0.25 mM EDTA-NaOH, pH 7.4 (320 mosM with sucrose). Pipettes of resistance 2–4 MΩ were used. An Axopatch 1D amplifier (Axon Instruments, Union City, CA) was used, and data were filtered at 1–2 kHz and digitized at 5–10 kHz. Recordings were made from NG108-15 cells 4 days after transfection/differentiation by using solutions designed to inhibit unwanted conductances, as described previously, and 20 mM Ba^{2+} was used as a charge carrier (10). Cells were clamped at a holding potential of –40 mV to eliminate low-voltage-activated Ca^{2+} currents. Recordings in *Xenopus* oocytes were made by using a two-electrode voltage clamp as described in ref. 11, with 2–40 mM Ba^{2+} as a charge carrier, as stated above. Analysis was performed by using the programs pclamp6 (Axon Instruments) and origin 7 (Microcal Software, Northampton, MA). Current records are shown following leak and residual capacitance current subtraction (P/4 or P/8 protocol). Individual current–voltage relationships were fitted with a modified Boltzmann equation: $I = G_{max}\,(V - V_{rev})/(1 + \exp[-(V - V_{50})/k])$, where G_{max} is the maximum conductance, V_{rev} is the reversal potential, k is the slope factor, and V_{50} is the voltage for 50% current activation.

1. Shi, J., Blundell, T. L. & Mizuguchi, K. (2001) *J. Mol. Biol.* **310,** 243–257.

2. Sali, A. & Blundell, T. L. (1993) *J. Mol. Biol.* **234,** 779–815.

3. Laskowski, R. A., MacArthur, M. W., Moss, D. S. & Thornton, J. M. (1993) *J. Appl. Crystallogr.* **26,** 283–291.

4. Provencher, S. W. & Glockner, J. (1981) *Biochemistry* **20,** 33–37.

5. Raghib, A., Bertaso, F., Davies, A., Page, K. M., Meir, A., Bogdanov, Y. & **Dolphin**, A. C. (2001) *J. Neurosci.* **21,** 8495–8504.

6. Altier, C., Dubel, S. J., Barrère, C., Jarvis, S. E., Stotz, S. C., Spaetgens, R. L., Scott, J. D., Cornet, V., De Waard, M., Zamponi, G. W., *et al.* (2002) *J. Biol. Chem.* **277,** 33598–33603.

7. Tomlinson, W. J., Stea, A., Bourinet, E., Charnet, P., Nargeot, J. & Snutch, T. P. (1993) *Neuropharmacology* **32,** 1117–1126.

8. Barclay, J. & Rees, M. (2000) *Mamm. Genome* **11,** 1142–1144.

9. Cormack, B. P., Valdivia, R. H. & Falkow, S. (1996) *Gene* **173,** 33–38.

10. Page, K. M., Heblich, F., Davies, A., Butcher, A. J., Leroy, J., Bertaso, F., Pratt, W. S. & **Dolphin**, A. C. (2004) *J. Neurosci.* **24,** 5400–5409.

11. Cantí, C., Page, K. M., Stephens, G. J. & **Dolphin**, A. C. (1999) *J. Neurosci.* **19,** 6855–6864.

12. Tinker, A., Jan, Y. N. & Jan, L. Y. (1996) *Cell* **87,** 857–868.

13. Marais, E., Klugbauer, N. & Hofmann, F. (2001) *Mol. Pharmacol.* **59,** 1243–1248.

14. Brice, N. L., Berrow, N. S., Campbell, V., Page, K. M., Brickley, K., Tedder, I. & **Dolphin**, A. C. (1997) *Eur. J. Neurosci.* **9,** 749–759.

15. Barclay, J., Balaguero, N., Mione, M., Ackerman, S. L., Letts, V. A., Brodbeck, J., Cantí, C., Meir, A., Page, K. M., Kusumi, K., *et al.* (2001) *J. Neurosci.* **21,** 6095–6104.

16. Brodbeck, J., Davies, A., Courtney, J.-M., Meir, A., Balaguero, N., Cantí, C., Moss, F. J., Page, K. M., Pratt, W. S., Hunt, S. P., *et al.* (2002) *J. Biol. Chem.* **277,** 7684–7693.

17. Moss, F. J., Viard, P., Davies, A., Bertaso, F., Page, K. M., Graham, A., Cantí, C., Plumpton, M., Plumpton, C., Clare, J. J., *et al.* (2002) *EMBO J.* **21,** 1514–1523.

18. Berrow, N. S., Brice, N. L., Tedder, I., Page, K. & **Dolphin**, A. C. (1997) *Eur. J. Neurosci.* **9,** 739–748.

19. Campbell, V., Berrow, N. S., Fitzgerald, E. M., Brickley, K. & **Dolphin**, A. C. (1995) *J. Physiol. (London)* **485,** 365–372.